Soft Matter

PAPER

Relationship between cooperative motion and the confinement length scale in confined colloidal liquids

Prasad S. Sarangapani,†*[a] Andrew B. Schofield[b] and Yingxi Zhu*[a]

The "confinement length scale", defined as the critical spacing where deviations from bulk behaviors begin, is widely examined with confined molecular and colloidal liquids, yet its origin and relationship to cooperative motion remain an open question. In this work, we examine the correlation between the sizes of cooperatively rearranging regions (CRRs) to the shift of "hard-sphere" colloidal glass transition in confined domains. We find that the confinement length scale observed in our prior work can be viewed as a regime where CRRs reach a finite size and sets the range for cooperative motion. Additionally, string-like motions within these mobile regions are enhanced at film thicknesses below the confinement length scale and reach maximal at the smallest thickness examined, suggesting an increase in the fragility of confined suspensions.

Introduction

The confinement effect on glass-forming liquids has received significant attention over the past two decades.[1–9] A number of studies have reported conflicting results, where the glass transition temperature, T_g, can increase,[2] decrease,[3] or remain roughly the same as the bulk T_g[4] depending on the nature of the surface treatment, however, there is little consensus regarding the physical interpretation of such observed phenomena.[1,2] A thorough understanding of the confinement effect on the glass transition is not only of fundamental importance to condensed matter physics, but also has far-reaching impact on diverse areas ranging from macromolecular crowding in cells[10] to sub-100 nm nanoimprint lithography.[11]

Prior work on confined glass-forming liquids has primarily focused on relating the critical dimension for the onset of confinement effects, known as the confinement length scale, to the sizes of cooperatively rearranging regions (CRRs), which may allow one to forge a direct connection with Adam-Gibbs theory.[2,5,9] Studies of planar polymer thin films have suggested that the cooperative dynamics near the air-polymer interface can perturb the underlying buried polymer layers, and the spatial extent of cooperative motion at the air-polymer interface thereby sets the confinement length scale for amorphous polymer thin films.[1,5] For glass formers confined in porous media,[1,2] studies of the relationship between pore size and CRR size have reported

conflicting results, indicating that confinement effects are pronounced when the pore size reaches the typical dimension of CRRs,[2] or show no impact on dynamic heterogeneity in glass-forming liquids.[1] In general, experimental studies that examine the relationship between confinement effects and CRRs are fraught with complications stemming from using model-dependent methods to extract dynamic length scales and the nature of surface conditions, which tend to vary significantly across studies. Computer simulations of the confinement effect in planar thin films and in porous media[5–8] have captured qualitatively similar behaviors as observed in experiments and provided an extra dimension by examining dynamic heterogeneity in confined thin films in detail and at a single-molecule or particle level. Earlier computer simulation studies[5–7] of super-cooled planar thin films have demonstrated that planar thin films can exhibit both faster and slower dynamics in confinement, implying that the sizes of CRRs decrease and increase, respectively, as film thickness is reduced. A more recent study of anti-plasticizer free thin films has shown a marked increase in the sizes of CRRs with decreasing film thickness.[8] Computer simulation of super-cooled liquids confined in nanopores has also attempted to give a precise relationship between the confinement length scale and the sizes of CRRs and predicted that the length scale associated with CRRs for glass formers confined in porous media is about 1/3 of the critical pore dimension for the onset of confinement effects,[12] which conflicts with the observations of prior experimental work.[5–8] In light of conflicting findings from experiments and computer simulations as well as the lack of direct experimental studies of the relationship between CRR size and confinement effects, it is of particular interest to examine the relationship between the confinement length scale and the sizes of CRRs in an experimental system where three-dimensional visualization of dynamics of confined glass-forming liquids at varied film thickness is possible.

[a]Dept. of Chemical and Biomolecular Engineering, University of Notre Dame, Notre Dame, IN, 46556, USA. E-mail: psaranga@alumni.nd.edu; yzhu3@nd.edu
[b]School of Physics, University of Edinburgh, Kings Buildings, Edinburgh, EH9 3JZ, UK
† Present Address: MedImmune, LLC, One Medimmune Way, Gaithersburg, MD 20878

"Hard-sphere" colloidal suspensions are well-studied model systems for molecular glass-forming liquids, where many experimental studies in the bulk and in confinement have captured the canonical behavior of glass forming liquids where key models of relaxation such as Adam-Gibbs and mode-coupling theories have been confirmed.[13–20] In our recent work on confined monodisperse hard-sphere colloidal liquids, we observed increasingly sluggish dynamics as film thickness is reduced, which is accompanied by a rapid increase of timescales for structural relaxation.[15] The confinement-induced glass transition is evident by the absence of a long time decay that is otherwise expected in equilibrium systems; similar glass-like behavior in confinement is also observed in confined suspensions of slightly polydisperse silica particles between rough walls[16] and confined binary hard-sphere colloidal suspensions.[17,18] Additionally, we have observed that the confinement length scale, which marks the onset of glass-like dynamics, occurs at progressively larger film thickness as volume fraction is increased, indicating that the critical volume fraction for colloidal glass transition, ϕ_g, decreases in confinement.[19] However, the origin of the confinement-induced glass transition and the relationship of the confinement length scale to cooperative motions remain open questions. In this work, we further extend our prior studies of confined hard-sphere colloidal liquids[15,19] and examine the correlations among the confinement length scale, string-like motion of mobile particles, and timescales for structural relaxation. The observed shift of the glass transition to lower volume fractions is intimately connected to the growing sizes of CRRs where the precipitous increase of relaxation times in confinement scales with film thickness in a similar manner as the string and cluster sizes, thus suggesting that the confinement length scale sets the range of cooperative motions.

Experimental

Our hard-sphere colloidal suspension consists of poly(methyl methacrylate) (PMMA) diameter, $d = 1.288$ μm, polydispersity <5%, sterically stabilized and impregnated with rhodamine 6G for direct visualization *via* confocal microscopy.[20] PMMA particles are suspended in dioctyl phthalate which matches the index of refraction of the particles ($n = 1.494$). Sedimentation is not observed for undisturbed samples for weeks. Volume fractions ranging from $\phi = 0.40$–0.57 with an uncertainty of ±0.03 are prepared and verified using Voronoi tessellation.[21,22] As in our previous work,[19] we find no deviations from the bulk volume fraction for the range of film thicknesses probed in our experiments. A home built micron-gap compression apparatus as previously described[19] is mounted on the stage of a confocal microscope (Zeiss LSM 5 Pascal, 100× objective, NA = 1.4) where film thickness, H is explored over a range of H/d from = 78 down to = 11. Boundary induced crystallization is prevented by spin-coating ~1–2 disordered layers of sterically stabilized PMMA particles (polydispersity ~ 18%) on each confining quartz surface and subsequently sintered at $T = 110$ °C for 40 min. A 10×10 mm^2 sample well is attached to the confining surfaces using UV-curing optical adhesive (Norland 80) and injected with ~200 μL of PMMA suspensions. We wait a minimum of five hours before commencing experiments to ensure transients have dissipated and prevent the formation of

depletion layers.[19] The protocol for confining samples is the same as our previous work.[19] Film thickness, H is determined solely from z-stacks with an accuracy of ±0.2 μm. A $30 \times 30 \times 12$ μm^3 volume containing ~3000 particles is scanned every 14 s for ~16 h. Three-dimensional particle centroiding algorithms[19] is subsequently employed to determine particle center positions with an accuracy of 0.05 μm in the x-y plane and 0.2 μm in the z-direction.

Results and discussion

We start by examining the film thickness dependence of structural relaxation for PMMA suspensions of $\phi = 0.40$ and 0.43 as shown in Fig. 1a–b, respectively, by measuring the overlap order parameter, $q_s(\tau)$, which is defined as

$$q_s(\tau) = \frac{1}{N} \sum_{i=1}^{N} w(|r_i(\tau) - r_i(0)|), \quad \text{(Eq. 1)}$$

where $w = 1(0)$ if $|r_i(\tau) - r_i(0)| < (>) a$, respectively. Thus, $q_s(\tau)$ quantifies the number of "overlapping" particles separated by a distance, a, compared within a time interval, τ, and thus
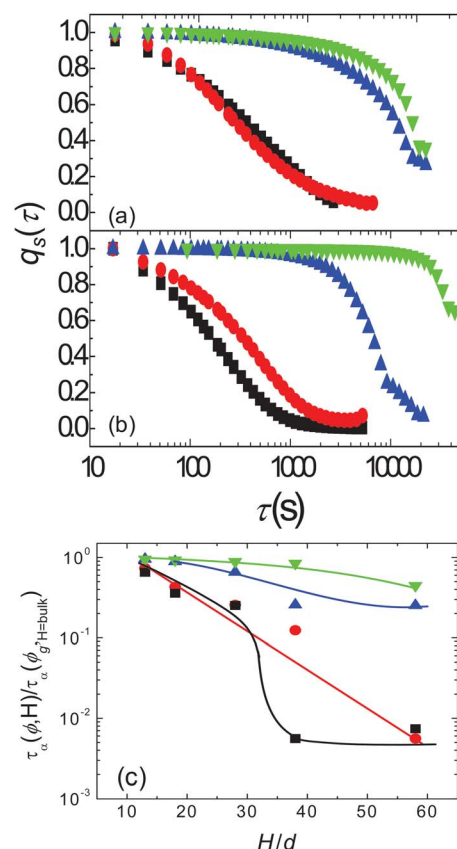

Fig. 1 Overlap order parameter, $q_s(\tau)$ for confined PMMA suspensions of $\phi = $ (a) 0.40 and (b) 0.43 at film thickness normalized by the diameter of PMMA particle, $H/d = 32$ (squares), 24 (circles), 15 (triangles), and 11 (inverted triangles). (c) H/d-dependence of relaxation time, τ_α, of confined PMMA suspensions of $\phi = 0.40$ (squares), 0.43 (circles), 0.46 (triangles), and 0.57 (inverted triangles) normalized by the relaxation time, $\tau_\alpha = 10,000$ s of the bulk PMMA suspension of $\phi = 0.58$. Solid lines are guides for eye.

provides a way to measure the localization of particle motion.[19] The parameter, a, is a "coarse graining" length scale that is larger than the typical vibration amplitude of particle motion in the β-regime. We find that a value of $a = 0.5d_{PMMA} = 0.65$ µm provides the best distinction between localized and delocalized particles in our system. It is evident in Fig. 1a–b that confinement has a strong effect on structural relaxation of confined colloids where the decay amplitude, defined as the timescale where $q_s(\tau) \sim 1/e$, grows in magnitude as H/d is reduced. A plausible interpretation of these data lies in examining the boundary conditions of our system, or alternatively speaking, the nature of the surface treatment: As we coat $\sim$1–2 layers of strongly polydisperse, sintered PMMA particles on each confining surface, the walls can be considered to be frozen and amorphous; consequently, the dynamics adjacent to the wall can become significantly slower than that in the interior of confined colloidal film, due to the enhanced particle-wall interactions,[17,18] resulting in the apparent glass-like dynamics of confined suspensions and a shift of the colloidal glass transition to lower volume fractions.

To explore the confinement-induced shift of the colloidal glass transition in hard-spheres, which occurs at $\phi = 0.58$ for monodisperse hard-sphere in bulk suspensions,[13] it is of interest to quantify the α-relaxation times, τ_α, extracted from the fitting of the overlap order parameter using the Kohlrausch-Williams-Watts formula as $q_s(\tau) = A\exp(-(\tau/\tau_\alpha)^\beta)$,[16,23,24] where A and β are freely floating fitting parameters for varied ϕ and H/d. We then normalize the obtained τ_α for confined suspensions by the relaxation time, $\tau_{\alpha, bulk} = 10,000$ s for a bulk PMMA hard-sphere colloidal glass of $\phi = 0.58$. Indeed, we find a strong thickness and volume fraction dependence of colloidal glass transition, where $\tau_\alpha/\tau_{\alpha, bulk}$ for the PMMA suspensions of $\phi = 0.46$ and 0.57 approach the unit at $H/d = 18$ and 28 respectively, signifying the dynamic arrest. On the contrary, suspensions of lower ϕ are ergodic even for thicknesses down to $H/d = 11$. These findings provide direct evidence of confinement-induced shift of colloidal glass transition to lower volume fractions, despite constant volume fraction at each thickness. It is noted that the critical thickness, at which the onset of structural arrest, i.e. $\tau_\alpha/\tau_{\alpha, bulk} \sim 1$, is observed, is estimated to be $H/d = 7$, 10, 18 and 28 for $\phi = 0.40$, 0.43. 0.46 and 0.57, respectively, as extracted from Fig. 1c. Compared to our previously reported confinement length scale of $(H/d)_{confinement} = 15$, 25, 40, 58 for respective $\phi = 0.40$, 0.43. 0.46 and 0.57,[19] the ϕ-dependence is consistent, yet the critical thicknesses for the onset of confinement effects obtained from Fig. 1c are generally smaller. We discuss this difference in greater detail below.

The interplay between boundary and finite-size effects is likely the cause for the increase in τ_α for structural relaxation in confined suspensions. As suggested by theory and simulation,[5–9] slow dynamics is typically accompanied by cooperative particle motions involving anomalously mobile particles. Therefore, it is of interest to examine whether clusters of *highly mobile* particles arise in confinement and correlate with the timescales associated with structural relaxation, τ_α. To examine this possibility, we choose the top 7% most mobile particles at each lag time, τ. This procedure,[25,26] on average, selects the particles that contribute to the tails of the probability distribution of displacements, $P(\Delta r, \tau)$. Clusters are identified as groups of mobile particles that are within the first neighbor shell of one another. Analysis of the

cluster statistics based on the probability distribution, $P_c(n,\tau)$, of cluster sizes at varied τ allows us to find the mean cluster size at varied τ by computing the weight-average cluster size,

$$\langle N_c \rangle = \frac{\sum_n n_c^2 P_c(n_c,\tau)}{\sum_n n_c P_c(n_c,\tau)}. \quad \text{(Eq. 2)}$$

It is also possible to compute the number-average cluster size, however, we choose to focus on the weight-average cluster sizes for our analysis simply because it captures the time dependent average cluster sizes in a representative manner. As the film thickness is reduced, spatio-temporal correlations between fast mobile particles increase and spatially extended large clusters appear as shown by the mean cluster size, $<N_c>$ in Fig. 2a–c for $\phi = 0.40$, 0.43 and 0.46, respectively, as well as the snapshots of mobile clusters at selected ϕ and H/d in Fig. 2d–f. It is particularly striking to find that very little change in the sizes of the clusters is detected for the suspensions of $\phi = 0.40$ and 0.43 even when the film thickness is reduced below their corresponding confinement length scale, $(H/d)_{confinement} = 15$ and 25.[19] Our results in Fig. 1 and 2 combined suggest that the critical thickness for the onset of confinement effects sets the size of CRRs, below which little change is observed in the measured τ_α; this is possibly true when we also consider the small change in the peak amplitude of $<N_c>$. To further strengthen this argument, we examine $<N_c>$ against τ for $\phi = 0.46$ and observe a precipitous increase in the peak amplitude in $<N_c>$ that is closely coupled with the
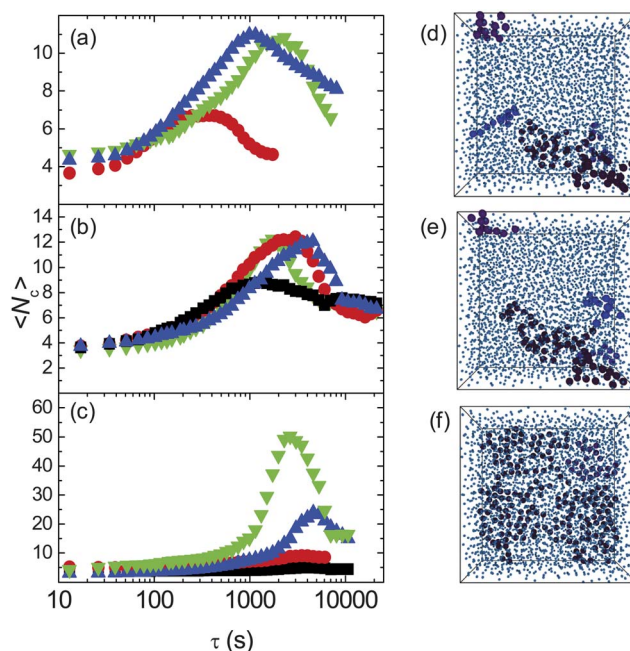

Fig. 2 Weight-averaged mobile cluster size, $<N_c>$ for confined PMMA suspensions of (a) $\phi = 0.40$ and at $H/d = 24$ (circles), 15 (triangles), 11 (inverted triangles), (b) $\phi = 0.43$ and at $H/d = 32$ (squares), 24 (circles), 15 (triangles), 11 (inverted triangles), and (c) $\phi = 0.46$ and at $H/d = 65$ (squares), 40 (circles), 23 (triangles), 18 (inverted triangles). Snapshots show the locations of mobile particles (large spheres) within CRRs that contain ten or more mobile particles and other particles (small spheres) at the peak amplitude in $<N_c>$ for (d) $\phi = 0.40$ and at $H/d = 11$, (e) $\phi = 0.43$ and at $H/d = 11$, and (f) $\phi = 0.46$ and at $H/d = 18$.

growing τ_α at reduced H/d as summarized in Fig. 1c. Significantly, structural arrest for $\phi = 0.46$ occurs at much larger H/d whereas the suspensions of $\phi = 0.40$ and 0.43 are still far from dynamic arrest.

To examine whether the clusters of mobile particles consist of replacing pairs of particles, or strings-like motions that exhibit quasi-1D motions,[9,25-27] we examine pairs of any two mobile particles, i and j and test whether they satisfy the following criteria: $\min[|r_i(t_0 + \tau) - r_j(t_0)|, |r_i(t_0) - r_j(t_0 + \tau)|] < \delta$, where $\delta = 0.97r_0$ and r_0 is the center-to-center distance between two mobile particles defined from the primary maximum in the pair-correlation function. This criterion ensures that if one mobile particle moves, an adjacent mobile particle will replace it within a radial distance of δ, and it is a definitive measure of string-like motion. Similar to the cluster analysis, the probability distribution of string sizes is expressed as $P_s(n, \tau)$, thus the mean string size at varied τ is quantified by calculating the weight-average string size as

$$\langle L_s \rangle = \frac{\sum\limits_n n_s^2 P_s(n, \tau)}{\sum\limits_n n_s P_s(n, \tau)}. \quad \text{(Eq. 3)}$$

As shown in Fig. 3a–c for $\phi = 0.40$, 0.43 and 0.46, respectively, the average string size, $\langle L_s \rangle$ grows as H/d is reduced; however, it should be noted that the maximum value of $\langle L_s \rangle$ never exceeds ~ 3 for varied ϕ. These trends are similar to the results obtained from computer simulations of fragile super-cooled Lennard-Jones liquids, where the average string length also never exceeds ~ 3 on timescales where $\langle L_s \rangle$ is peaked.[9,27] As displayed in Fig. 3d–f for selected ϕ and H/d, snapshots of the strings of

mobile particles around the peak amplitude of $\langle L_s \rangle$ reveals that a non-trivial fraction of strings consist of compact closed loops, yet most strings appear to be ramified in space and "chain-like" in nature.

From the analysis of CRRs and strings above, it is clear that the observed slow dynamics in confinement is due to the growing sizes of CRRs and enhanced string-like motions within CRRs. In general, one may expect that due to confinement, the lateral dynamics are significantly faster than the dynamics normal to the walls, as shown in our previous study *via* mean-square displacements[15,19] and related studies by other researchers;[16,18] therefore, it is reasonable to consider that the mobile particles have a preferred orientation parallel to the walls to facilitate structural relaxation under the influence of strong confinement.[18] To examine whether this is the case for confined hard-sphere glasses, we utilize a simple yet powerful method to examine how the orientation of strings in confinement is coupled with the observed slow dynamics by labeling mobile particles that are involved in string-like motions according to their displacements in the z-direction. As shown in Fig. 3d–f for $\phi = 0.40$–0.46 at varied H/d, we find that most strings are instead normal to the walls; this suggests that the shapes of CRRs are not necessarily "flattened" in confinement, at least not over the range of film thicknesses we examined in this work, which is consistent with another recent study.[18] Therefore we consider that most strings are possibly formed by inter-layer exchange of the positions of mobile particles, which results in long-ranged facilitated glass-like dynamics in confinement.

The results above merit a more comprehensive discussion of the influence of boundary conditions on the orientation of CRRs in confinement. Prior work[17,18] on dynamic heterogeneity in confined binary hard-sphere colloidal liquids using smooth, untreated walls has demonstrated the layering of CRRs as film thickness approaches the particle diameter is resulted from the presence of flat patches and separated by immobile particles adhering to the surface; consequently, structural relaxation in such confined colloidal liquids is dominated by the mobile particles that are free to move laterally between the layers.[18,27] However, the confining walls in our experiments are uniformly roughened and instead, the layering of mobile particles is never observed. Therefore, in our case, under strong confinement at small film thickness where slow dynamics is pronounced, CRRs are not constrained to lateral motion or "flattened". The influence of boundary conditions are thus non-trivial when examining the glassy behavior in confined glass-forming liquids, which could create greater subtlety to the problem in comparison to the study of the glass transition in the bulk.

Finally, to probe the correlation between timescales for structural relaxation, the confinement length scale, and the size of CRRs, it is of interest to examine the scaling of the mean cluster size, $\langle N_c \rangle$ and mean string size, $\langle L_s \rangle$ with H/d on timescales where these quantities are maximal, as summarized in Fig. 4a–b, respectively. A comparison of Fig. 1c to Fig. 4a–b shows that $\langle N_c \rangle$ and $\langle L_s \rangle$ closely follow τ_α, confirming that anomalously mobile particles are primarily responsible for structural relaxation in confined suspensions. It is also interesting to note that the thickness range where the sizes of mobile clusters and strings exhibit a rapid increase correlates well with the previously reported confinement length scales,[19] thus
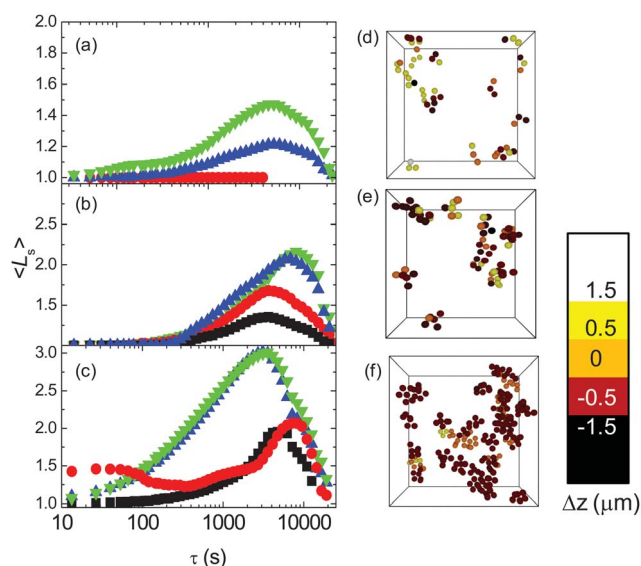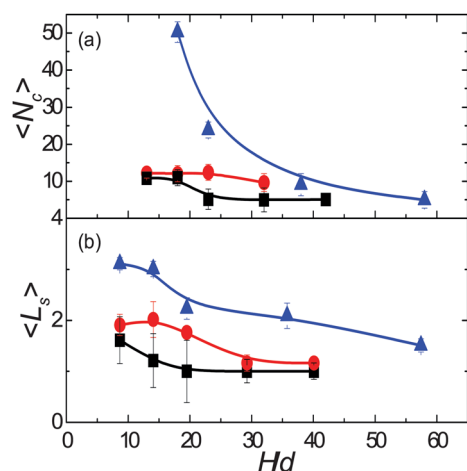

Fig. 3 Weight-averaged string size, $\langle L_s \rangle$ for confined PMMA suspensions of (a) $\phi = 0.40$ and at $H/d = 24$ (circles), 15 (triangles), 11 (inverted triangles), b) $\phi = 0.43$ and at $H/d = 32$ (squares), 24 (circles), 15 (triangles), 11 (inverted triangles), and c) $\phi = 0.46$ and at $H/d = 65$ (squares), 40 (circles), 23 (triangles), 18 (inverted triangles). Snapshots show the orientation of "strings" in confinement at a timescale where $\langle L_s \rangle$ is maximal for (d) $\phi = 0.40$ and at $H/d = 11$, (e) $\phi = 0.43$ and at $H/d = 11$, and (f) $\phi = 0.46$ and at $H/d = 18$. Particles are labeled according to their displacement in the z-direction as indicated in the color bar.

Fig. 4 Scaling of the maximal value of (a) $\langle N_c \rangle$ (closed symbols) and (b) $\langle L_s \rangle$ (open symbols) with H/d for confined PMMA suspensions of $\phi = 0.40$ (squares), 0.43 (circles) and 0.46 (triangles).

suggesting that the confinement length scale represents a regime where strong spatially heterogeneous dynamics manifests. Taken together, these trends qualitatively suggest that the fragility of confined suspensions increases as the film thickness is reduced, and the increased fragility is coupled with the precipitous slowing-down of dynamics over a very narrow range of film thickness.

Conclusion

In summary, we have examined the confinement effect on cooperative motion and find non-trivial correlations between the timescales of structural relaxation and the sizes of CRRs, which is intimately connected to the reduction of the critical volume fraction, ϕ_g for the onset of colloidal glass transition. It is interesting to observe that for $\phi = 0.40$ and 0.43, the sizes of CRRs show little change at $H/d \leq 15$, which is smaller than the previously reported confinement length scales for confined PMMA suspensions at the same corresponding ϕ. This behavior suggests that once the CRRs reach a critical size, slow dynamics arises and more significantly, the confinement effect on particle dynamics becomes weaker as film thickness is further reduced. Conversely, the average string sizes show a strong thickness dependence, where string-like motions, on average, are pronounced at the smallest thickness, implying that the fragility of colloidal hard-sphere suspensions increases with stronger confinement. A potentially interesting future study could involve tuning the fragility of colloidal suspensions to deduce the precise relationship between fragility, confinement length scale, and string-like cooperative motion in confinement.

References

1 M. Alcoutalbi and G. B. McKenna, *J. Phys.: Condens. Matter*, 2005, **17**, R461–R524.
2 R. Richert, *Phys. Rev. B: Condens. Matter*, 1996, **54**, 15762–15766.
3 H. Sillescu, *J. Non-Cryst. Solids*, 1999, **243**, 81–108.
4 C. B. Roth and J. M. Torkelson, *Macromolecules*, 2007, **40**, 3328–3336.
5 C. J. Ellison and J. M. Torkelson, *Nat. Mater.*, 2003, **2**, 695–700.
6 F. Varnik, J. Baschnagel and K. Binder, *Phys. Rev. E: Stat. Phys., Plasmas, Fluids, Relat. Interdiscip. Top.*, 2002, **65**, 0215071–02150714.
7 J. Baschnagel and F. Varnik, *J. Phys.: Condens. Matter*, 2005, **17**, R851–R953.
8 C. Bennemann, J. Baschnagel and W. Paul, *Eur. Phys. J. B*, 1999, **10**, 323–334.
9 R. A. Riggleman, K. Yoshimoto, J. F. Douglas and J. J. de Pablo, *Phys. Rev. Lett.*, 2006, **97**, 045502–045505.
10 H. X. Zhou, G. N. Rivas and A. P. Minton, *Annu. Rev. Biophys.*, 2008, **37**, 375–397.
11 Y. Ding, H. W. Ro, T. A. Germer, J. F. Douglas, B. C. Okerberg, A. Karim and C. L. Soles, *ACS Nano*, 2007, **1**, 84–92.
12 P. Scheidler, W. Kob and K. Binder, *J. Phys. Chem. B*, 2004, **108**, 6673–6686.
13 E. R. Weeks and D. A. Weitz, *Phys. Rev. Lett.*, 2002, **89**, 095704–095707.
14 A. H. Marcus, J. Schofield and S. A. Rice, *Phys. Rev. E: Stat. Phys., Plasmas, Fluids, Relat. Interdiscip. Top.*, 1999, **60**, 5725–5736.
15 P. S. Sarangapani and Y. Zhu, *Phys. Rev. E: Stat., Nonlinear, Soft Matter Phys.*, 2008, **77**, 010501R.
16 H. B. Eral, D. van den Ende, F. Mugele and M. H. G. Duits, *Phys. Rev. E: Stat., Nonlinear, Soft Matter Phys.*, 2009, **80**, 061403.
17 C. R. Nugent, K. V. Edmond, H. N. Patel and E. R. Weeks, *Phys. Rev. Lett.*, 2007, **99**, 025702.
18 K. V. Edmond, C. R. Nugent and E. R. Weeks, *Eur. Phys. J. Spec. Top.*, 2010, **189**, 83–93.
19 P. S. Sarangapani, A. B. Schofield and Y. Zhu, *Phys. Rev. E: Stat., Nonlinear, Soft Matter Phys.*, 2011, **83**, 030502.
20 A. D. Dinsmore, E. R. Weeks, V. Prasad, A. C. Levitt and D. A. Weitz, *Appl. Opt.*, 2001, **40**, 4152–4159.
21 F. Preparata and M. I. Shamos, *Computational Geometry*, Springer-Verlag, 1985.
22 N. Lacevic, F. W. Starr, T. B. Schroeder and S. C. Glotzer, *J. Chem. Phys.*, 2003, **119**, 7372–7387.
23 J. T. Bendler and M. F. Shlesinger, *Macromolecules*, 1985, **18**, 591–592.
24 G. Brambilla, D. El Masri, M. Pierno, L. Berthier, L. Cipelletti, G. Petekidis and A. B. Schofield, *Phys. Rev. Lett.*, 2009, **102**, 085703.
25 M. Vogel and S. C. Glotzer, *Phys. Rev. Lett.*, 2004, **92**, 255901–255904.
26 E. R. Weeks, J. C. Crocker, A. C. Levitt, A. Schofield and D. A. Weitz, *Science*, 2000, **287**, 627–631.
27 C. Donati, J. F. Douglas, W. Kob, S. J. Plimpton, P. H. Poole and S. C. Glotzer, *Phys. Rev. Lett.*, 1998, **80**, 2338–2341.